Journal of Computers Vol. 34 No. 3, June 2023, pp. 315-324
doi: 10.53106/199115992023063403023

Research on Intelligent Assembly Strategy and Workpiece Grasping Method for Industrial Robots Based on Deep Learning

Jie Yu, Xi-Lin Li*, Cai-Wen Niu, Yu-Xin Zhang, Shu-Hui Xu

School of Automation Engineering, Tangshan Polytechnic College,
Tangshan City 063000, Hebei Province, China
{yujie32543, xilin32987, tgy511389410, yuxin8765, shuhui123}@163.com

Received 1 March 2023; Revised 1 April 2023; Accepted 17 May 2023

Abstract. In response to the current situation of low assembly accuracy and unreasonable workpiece grasping posture in the automatic assembly process of equipment manufacturing based on industrial robots, an objective function was designed with the goal of minimizing robot grasping torque, and a deep learning strategy was used to autonomously identify the optimal grasping posture. In terms of assembly strategy selection, the assembly behavior is abstracted as the coordination between holes and shafts. A method of changing the center distance of shaft hole parts to change the jamming state of holes and shafts is proposed to increase the assembly qualification rate. Finally, the industrial robot in the training base is used as the experimental object to validate the method proposed in this paper. After comparative analysis, the proposed method increases the assembly efficiency by 10.4%, and the assembly success rate reaches 96%.

Keywords: deep learning, assembly strategy, machine vision, convolutional neural network

1 Introduction

For a device, the final stage of design and manufacturing is assembly. How to maximize the design performance of the device is crucial in the assembly process. The development of industrial robots is gradually changing production and labor methods. With the deeper and wider development of industrial robots and the improvement of robot intelligence level, the application scope of robots is constantly expanding, and has been promoted from the automotive manufacturing industry to other manufacturing industries, and to various non manufacturing industries such as mining robots, construction robots, and water and electricity system maintenance and repair robots. The use of industrial robots to grab workpieces and assemble them is the current development direction in the field of assembly, but robots have the following problems in the assembly process:

(1) The accuracy of workpiece grasping is insufficient, and incorrect workpiece grasping directly leads to assembly errors;

(2) The position and posture of workpiece grasping are unreasonable, increasing assembly errors and difficulty, as well as adding useless paths for assembly;

(3) Insufficient assembly accuracy leads to a decrease in equipment accuracy and the loss of significance for robot assembly.

Automatic assembly can be divided into two main issues: first, achieving precise target and target pose grasping, and second, completing precise assembly. Therefore, the main work completed in this article is as follows:

(1) Studied the robot grasping strategy and established an optimization objective function based on the grasping torque;

(2) Abstract the assembly object as a hole axis assembly, and establish an artificial intelligence assembly strategy based on the stuck state of the hole axis and deep learning algorithm.

In order to comprehensively discuss the work done, the chapter structure of this article is arranged as follows:

Chapter 2 searched for the research results of relevant scholars on the issues raised in this article, and conducted corresponding analysis and comparison. Chapter 3 discussed the robot grasping strategy based on vision. Chapter 4 determined the assembly strategy based on the blockage of the hole axis. Chapter 5 mainly focused on experimental analysis and analyzed the advantages of this method. Chapter 6 was the conclusion section.

* Corresponding Author

2 Related Work

Relevant scholars have conducted research on assembly strategies and determined the research direction of this article through comparative analysis. Alles studied the assembly strategy of dual arm robots and proposed a modular method to implement the shaft hole assembly strategy. At the same time, the accuracy and stability of the model were demonstrated under different assembly gaps. The research on assembly gaps is of reference significance for this article [1]. Nottensteiner proposed a robot assembly method that combines visual and internal tactile perception, and achieved the robot's ability to continuously track parts within a single Bayesian framework, And the feasibility of the method was confirmed through hole axis matching, and the application of vision provides a reference for this article [2]. Kamal proposed to carry out motion planning for the end effector of the robot, so as to conduct Peg-In-Hole search with the minimum prior information of the working environment, which can enable the robot to work with the minimum prior information of the working environment to eliminate any interference in the assembly process [3]. Peng Liu designed an automation system and mainly planned the implementation path for the automatic locking screw assembly task in response to the problems of low work efficiency and low level of automation in screw assembly [4]. Zhe Li proposed a robotic arm workpiece grasping scheme that utilizes a new fast expanding random tree algorithm and visual positioning to address the potential collisions that may occur in the environment, improving the accuracy and stability of part grasping [5]. Yuexin Tian proposed a 3D visual recognition and grabbing system based on deep learning method, which achieves grabbing errors within 1-4 mm. The algorithm is highly feasible, but the grabbing accuracy is low [6].

3 Visual Based Workpiece Grasping Model for Industrial Robots

Any assembly process can be abstracted as the coordination of holes and shafts, and the completion of shaft hole assembly tasks by industrial robots generally includes the following two stages: workpiece grasping and workpiece assembly. This chapter mainly studies the grasping process of industrial robots. In addition to discussing the accuracy of workpiece grasping, it also discusses the method of correctly grasping the position of the workpiece. This chapter mainly analyzes the factors that affect assembly accuracy, and then uses deep learning methods to find the optimal assembly plan.

3.1 The Influence of Workpiece Grasping Angle

During the assembly process, there is a certain insertion angle between the hole axes. If the insertion angle is within a reasonable range, the insertion action can be completed. However, excessive inclination angle can lead to the failure of the shaft hole assembly [7]. Therefore, the inclination angle during the hole axis assembly process is a key parameter in the assembly process. Set the maximum inclination angle between the hole axes as α, as shown in Fig. 1.

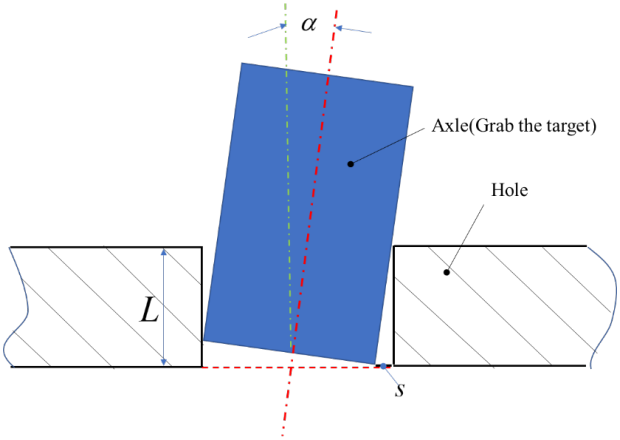

Fig. 1. Schematic diagram of hole axis inclination angle

The inclination angle A can be expressed as:

$$\alpha = \arctan\frac{s}{L}. \tag{1}$$

According to Fig. 1 and Formula 1, the larger the tilt angle α is, the larger the assembly clearance s is, while the insertion distance L is inversely proportional to the tilt angle. When the actual assembly angle is greater than the tilt angle α , the assembly task cannot be completed. Therefore, the main adjustment goal of industrial robots in the assembly process is to make the assembly angle less than the maximum allowable tilt angle.

3.2 The Torque Generated During the Grasping Process

The generation of grasping torque depends on the position of the robot gripper grasping the parts, and different grasping torques will cause different disturbances and motion trajectories, ultimately leading to different assembly differences. At the same time, the interference generated by the torque during the adjustment of the axis hole alignment of the robot is also constantly changing, so the grasping torque is also the main influencing parameter. The interference torque includes the gravity torque M_G and inertia torque M_I of the workpiece, and their respective expressions are as follows:

$$M_G = mg|s|\sin\theta. \tag{2}$$

$$M_I = J\delta = \frac{1}{2}mr^2\frac{d^2\lambda}{dt^2}. \tag{3}$$

Among them, m is the mass of the assembly axis, g is the acceleration of gravity, s is the distance from the point of force application to the axis of rotation, and θ is the angle between the moment of gravity and the force. δ is the angular acceleration, ω is the angular velocity, J is the moment of inertia, r is the vertical distance between the center of mass and the center of rotation, λ is the angular displacement, where the moment of inertia J and angular acceleration δ are expressed as:

$$J = \frac{1}{2}mr^2. \tag{4}$$

$$\delta = \frac{\omega}{t} = \frac{d^2\lambda}{dt^2}. \tag{5}$$

From the above formula, it can be seen that the generation of interference torque is mainly influenced by the quality of the assembly shaft and the distance and angular displacement generated by the gripping position of the assembly shaft. When the grasping position coincides with the center of mass and the center of rotation, the action distance is the smallest, so the gravitational interference torque generated during the adjustment process is also the smallest. When the grasping position is not only at the position where the center of mass coincides with the center of rotation, but also at the position where the inertial axis coincides with the rotation axis, the robot generates the minimum gravity interference torque and inertial interference torque during the assembly process. Therefore, when selecting the gripping position with smaller interference torque, the interference received during the assembly process is smaller, which is more conducive to the completion of the assembly task.

3.3 A Grasping Strategy for Industrial Robots Based on Deep Learning

This section mainly studies the establishment of a mapping relationship between grasping position and assembly efficiency constraints through self-supervised deep learning training, enabling robots to autonomously search for

the optimal grasping position to reduce the impact of interference torque on completing subsequent assembly tasks.

The control system regards the grasping decision process as a Markov decision process [8], and the state action reward chain during the grasping process can be expressed as:

$$\{s_0, a_0, R_0, s_1, a_1, R_1, s_2 \cdots, s_{t-1}, a_{t-1}, R_{t-1}, s_t\}. \tag{6}$$

Among them, s_t represents the environmental state perceived by t at all times. Using strategy $\pi(s_t)$, feasible action a_t is selected from the available action set $A(s)$. After the robot executes the action, the environmental state changes from s_t to s_{t+1}, and a reward $R(s_t, s_{t+1})$ is obtained. This reward is composed of grasping reward r_{t+1}^G and assembly reward r_{t+1}^{AM}. The robot receives a reward $r_t^G = 0.3$ after each successful grasping. When the grasping position is selected, if the assembly time is less than the set time threshold, it receives assembly reward $r_t^{AM} = 0.7$. Therefore, The formula for rewarding $R(s_t, s_{t+1})$ is described as follows:

$$R(s_t, s_{t+1}) = r_t^G + r_t^{AM}. \tag{7}$$

When selecting to perform assembly actions, the robot evaluates the value $Q(a)$ of each action in action set $A(s)$, selects the most valuable execution action a_t, and adds assembly reward r^{AM}. The robot establishes a mapping relationship between the grasping position and assembly work efficiency to achieve maximum reward. When the robot obtains the maximum reward reward, if the assembly time of the robot meets the assembly task constraints, it proves that this strategy can improve the assembly efficiency of the robot and achieve the goal of learning intelligent visual grasping skills. Therefore, the action value function is expressed as:

$$Q_\pi(S_t, A_t) = E_\pi\left[G_t \middle| S_t = s, A_t = a\right] = E_\pi\left[\sum_{k=0}^{\infty} \gamma^k R_{t+k+1} \middle| S_t = s, A_t = a\right]. \tag{8}$$

The optimal value function is expressed as:

$$Q^*(s_t, a_t) = \max_\pi Q_\pi(s_t, a_t) = R(s_t, a_t) + \gamma \max_{a \in A(s)} Q_\pi(s_{t+1}, a_{t+1}). \tag{9}$$

The robot obtains the optimal strategy π^* through training, and the trained optimal strategy π^* can select the highest predicted Q value and optimal action a_t^* from the feasible action set under the current state s_t of time *t*. The formula for obtaining the optimal strategy π^* is as follows:

$$\pi^*(s_t) = \arg\max_{a \in A(s)} Q^*(s_t, a_t) = \arg\max_{a \in A(s)} E\left[R(s_t, a_t) + \gamma Q_\pi^*(s_{t+1}, a_{t+1})\right]. \tag{10}$$

3.4 Decision Neural Network for Workpiece Grasping

The robot observes environmental information through a fixed installation of realistic depth cameras, and then the visual perception system projects the perceived RGB image information and depth information data onto a 3D point cloud, and constructs a height map with RGB D channel information through orthogonal backprojection in the gravity direction. The system inputs the color channel (RGB) and cloned depth channel of the height map into Resnet pre trained on Imagnet for image feature processing. Then, the network sends image features to two convolution units for data processing. The convolution unit consists of activation function layer (ReLU) and convolution layer [9]. The robot will select the executable action a_t^* with the highest Q value in the predicted heat map as the current execution action. The neural network structure for grasping decisions is shown in Fig. 2.

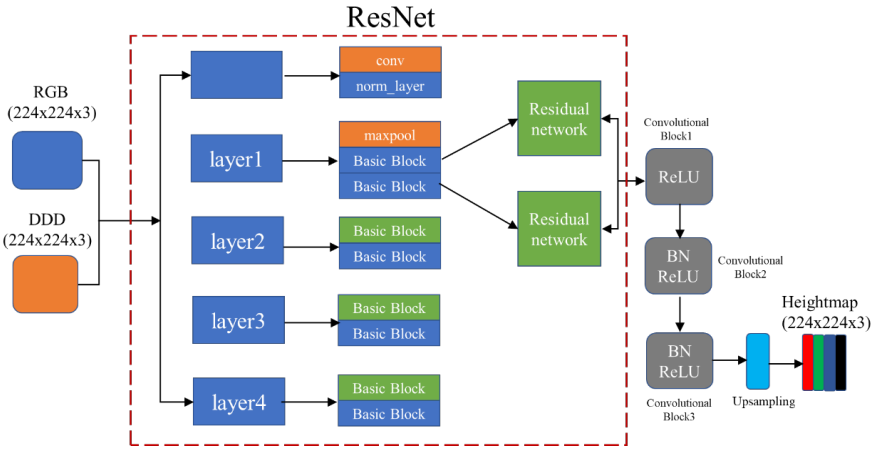

Fig. 2. Grasping decision neural network structure

The crawling decision neural network is a fully convolutional neural network constructed based on DQN [10]. DQN is a learning method that combines neural networks and Q-learning. The traditional reinforcement learning Q-learning method stores the Q-values of each state and each executable action in that state in the Q-lattice. The fully convolutional neural network uses bilinear upsampling to increase the resolution of the feature map in order to output a pixel level predicted heat map of the same size as the input image, thereby achieving the restoration of the input image size and resolution. Bilinear upsampling uses a bilinear interpolation algorithm to insert new elements between the pixels in the current feature map, which estimates the pixel color lost in the original image based on the existing pixels in the feature map. To facilitate the description, the input feature map is defined as the initial feature map, and the upsampled feature map is defined as the expected feature map. The coordinate transformation formula for two feature maps is:

$$x_0 = x_e \times \left(\frac{w_0}{w_e} \right). \tag{11}$$

$$y_0 = y_e \times \left(\frac{h_0}{h_e} \right). \tag{12}$$

Among them, x_e is the x -axis coordinate value of the expected feature map, w_0 is the initial feature map width, w_e is the expected feature map width, x_0 is the x -axis coordinate of the initial feature map corresponding to the coordinate transformation, y_e is the y -axis coordinate value of the expected feature map, h_0 is the initial feature map height, h_e is the expected feature map height, and y_0 is the L-axis coordinate of the initial feature map corresponding to the coordinate transformation. In order to ensure the image accuracy after feature map transformation, the neural network uses bilinear interpolation algorithm to calculate the pixel values of the corresponding pixel points of the expected feature map based on the pixel values of four real pixel points near the virtual points in the initial feature map. After calculation by the bilinear interpolation algorithm, the image resolution is expanded to the expected size based on the initial feature map, as shown in Fig. 3. The calculation expression for bilinear interpolation is as follows:

$$\begin{aligned} f(i+u, j+v) &= (1-u)(1-v) f(i, j) + (1-u) v f(i, j+1) + \\ & u(1-v) f(i+1, j) + uv f(i+1, j+1). \end{aligned} \tag{13}$$

i, j is the integer part of the transformation coordinate, $f(i, j)$ is the pixel value of the initial feature map (i, j) coordinate, and u, v is the decimal part of the transformation coordinate, with a value range of $[0, 1)$. The sampling schematic diagram on the system is shown in Fig. 3.

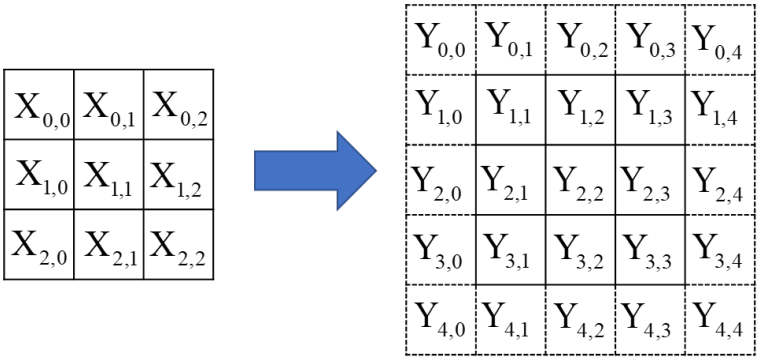

Fig. 3. Schematic diagram of upsampling

ReLU activation function uses unilateral inhibition to add sparse activation to neurons in the network, thus solving the problem of gradient explosion and gradient disappearance, and has a fast network training convergence speed. In addition, ReLU activation function does not involve power operation, which greatly reduces the operation cost. The ReLU activation function formula is:

$$f(x) = \max(0, x) = \begin{cases} 0 & (x \le 0) \\ x & (x > 0) \end{cases}. \tag{14}$$

4 Axis Hole Assembly Strategy

To complete the assembly of small clearance shaft holes, the deviation of the included angle α of the part axis must be less than 0.5. Within the allowable range of grasping angle, the assembly strategy proposed in this paper is proposed to reduce interference caused by tilt angle, torque disturbance, etc. After the parts come into contact, only changing the distance between the center of the shaft hole parts will transition the parts from a radial jamming state to a bidirectional jamming state, and then cause the parts to move along the bidirectional jamming state function curve, keeping the parts in a bidirectional jamming state until the shaft hole assembly is completed [11]. The stuck state is shown in Fig. 4.

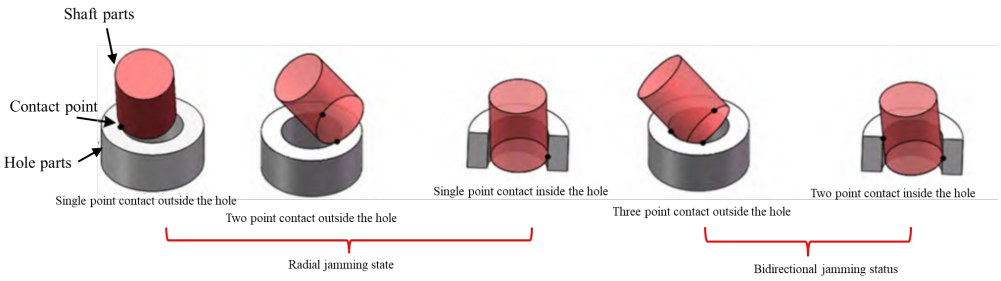

Fig. 4. Contact status of shaft hole assembly

The advantage of this assembly strategy is that even if there is excessive rotation during the assembly process of the shaft parts, they can be translated in reverse and re moved to a new bi-directional jamming state. Among them, the relationship between the horizontal and vertical displacement Δl and Δh of the robot per unit time and the rotation angle $\Delta\alpha$ per unit time can be expressed by the following formula:

$$\begin{cases} \triangle h = \dfrac{D - d \times \cos(a + \triangle a)}{\sin(a + \triangle a)} - \dfrac{D - d \times \cos(a)}{\sin(a)} \\ \triangle l = \dfrac{d}{2} \times \left[\cos(a + \triangle a) - \cos(a)\right] + H \times \left[\sin(a + \triangle a) - \sin(a)\right] \end{cases} . \tag{15}$$

The various parameters used in the assembly of industrial robot shaft holes are shown in Table 1, and the assembly strategy process is as follows:

Step 1: Prepare points for robot motion value assembly;

Step 2: Zero the force sensor and initialize the assembly operation parameters.

Step 3: The robot slowly descends Δh along the assembly direction until preliminary contact is made with the shaft hole, entering an axial jamming state. Condition 1 is met, and the reading N_Z of the force sensor Z axis is greater than a certain threshold F_Z.

Step 4: Take the readings of the X and Y axes of the force sensor, obtain the direction and magnitude of the resultant force F at the end contact point, and make the robot translate Δl along this direction. During the translation process, keep the reading N_Z of the sensor Z axis greater than the threshold F_Z at all times, until the axis parts enter a bidirectional jamming state, that is, meet condition 2: the difference $M_{X,Y}$ between the front and back times is greater than the threshold $\Delta M_{X,Y}$.

Step 5: Record the insertion depth h' at this time, and use formula 15 to calculate the angle α between the axes as the initial value of the angle. The robot starts to move and uses an admittance controller for displacement compensation until condition 3 is met: the depth h of the axis insertion hole is greater than h_z.

Table 1. Process parameter table

Parameter symbols	Parameter meaning
$\triangle h$	Descending distance
N_Z	Sensor Z-axis reading
F_Z	Sensor Z-axis threshold
$M_{X,Y}$	Bidirectional clamping torque
$\triangle M_{X,Y}$	Change value of bidirectional clamping torque
$T_{X,Y}$	Threshold of bidirectional card resistance moment
$h^{'}$	Record value of shaft insertion hole depth
α	Axis hole inclination angle
h	Current insertion depth value
h_Z	Axis insertion hole depth threshold

In actual operation, during the assembly process of the shaft hole, the parts are in rigid contact and the assembly clearance is minimal. After the force sensor data F_s and T_s are calibrated and gravity compensated, the assembly contact forces F_c and T_c are obtained. The expected forces F_d and T_d are calculated from the robot's actual positions and postures X_s and θ_s, and then they are input into the admittance controller to obtain the compensation positions and postures X_c and θ_c, and the theoretical assembly positions and postures X_d and θ_d are compensated. The motion of each axis of the robot is controlled by inverse kinematics and PID controllers. The control system schematic diagram is shown in Fig. 5.

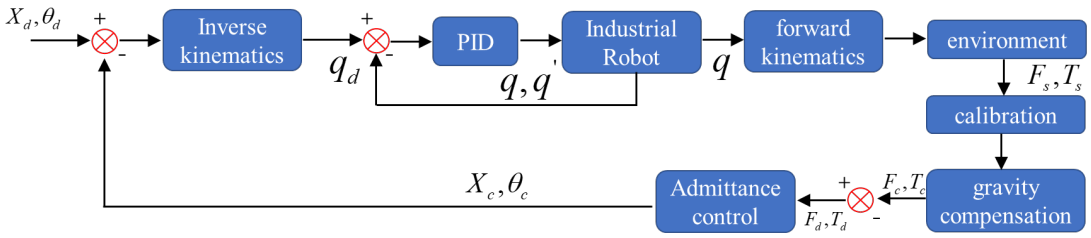

Fig. 5. Control system diagram

5 Experimental Results and Analysis

In order to verify the feasibility and effectiveness of the shaft hole assembly strategy based on deep reinforcement learning and proposed in this article, a robot physics experimental platform was established for workpiece grasping and assembly strategy testing. As shown in Fig. 6, the KUKA robot is equipped with force/torque sensors, pneumatic grippers, and visual sensors.

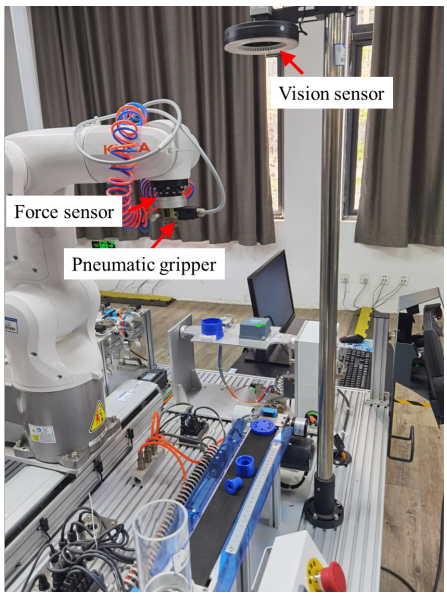

Fig. 6. Robot experimental platform

Table 2 shows the assembly objects for this time.

Table 2. Assembly object parameters

Nominal diameter of shaft hole	Assembly depth	Minimum clearance of shaft hole	Center distance deviation	Shaft angle
25mm	21mm	0.21mm	0-15mm	≤8°

To verify the effectiveness of this assembly strategy, a robot was used to repeatedly grasp the workpiece for 500 assembly experiments with shaft hole matching. The main criterion for determining the success of the robot's grasping strategy is the change in assembly time. If the grasping position is more reasonable, the assembly time will be less. The total time required for the deep learning based grasping strategy and shaft hole assembly

method proposed in this article is 3.38 hours. Compared to the previous assembly strategy of 4.02 hours, it saved 0.64 hours and increased work efficiency by 15.9%. In order to more intuitively reflect the differences in assembly time after the improvement strategy, 50 sets of data from the test samples were selected for comparison, and the comparison results are shown in Fig. 7.

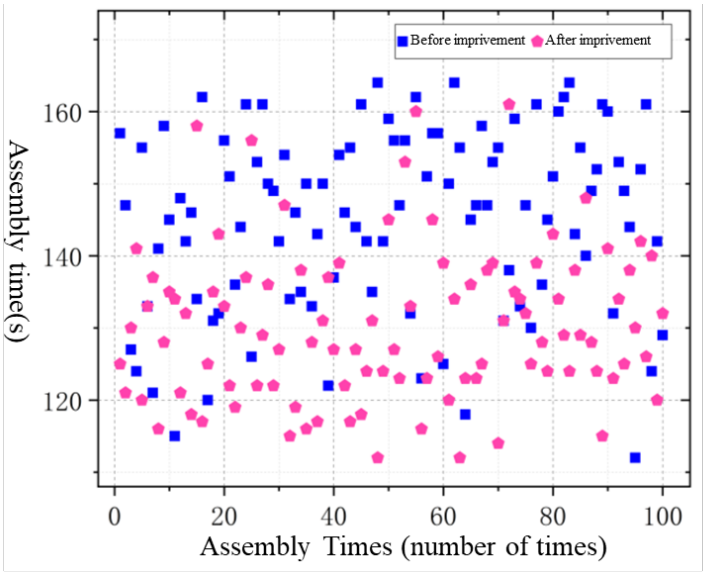

Fig. 7. Robot experimental platform

In this 50 assembly process, the initial pose deviation of the parts was random in each experiment, and the reading of the force sensor during the experiment was recorded. When the reading of the force sensor was greater than 50N, it was considered an experiment failure. Fig. 8 shows the success and failure of the proposed strategy in this article under different center distance deviations and axis angles of the parts. In a total of 50 experiments, there were 2 assembly failures, with an assembly success rate of 96%.

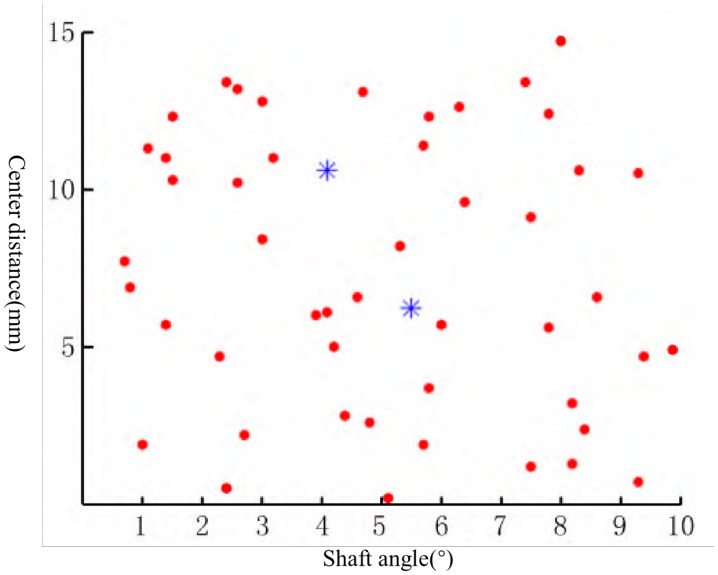

Fig. 8. Assembly results of hole shaft

The experimental results show that gravity interference torque and inertia torque have the most significant impact on the fluctuation of interference torque among numerous interference torques. This article introduces assembly rewards for grasping decision-making and establishes a mapping relationship between grasping position and assembly efficiency to limit the selection of grasping position and reduce the fluctuation of assembly time. In order to verify the feasibility and generalization of the strategy, this chapter conducted robot simulation analysis and experimental research on shaft hole assembly. The experimental data showed that using intelligent visual grasping strategy can improve the assembly efficiency of the robot by 10.4%. At the same time, in the single assembly process, this strategy ensures accurate and stable contact motion during the actual assembly process, reducing the repeated pose adjustment process, resulting in a success rate of 96% in the case of small samples and large positioning deviation, an average completion time of 15.1 seconds, and an average maximum contact force of 14.8N.

6 Conclusion

This article establishes a robot vision based workpiece grasping model and uses deep learning to automatically learn the optimal assembly strategy. After experimental verification, the assembly efficiency has been improved by 10.4%, and the assembly success rate has reached 96%. The effectiveness of the algorithm has been verified. For this reason, further research focuses on more complex assembly scenarios, as most assembly scenarios are abstracted as hole axes, while in reality, there are scenarios that cannot be abstracted as hole axes, such as flange facing assembly.

7 Acknowledgement

Exploration and practice of improving curriculum ideological and political ability of electromechanical teachers in higher vocational colleges (TSSKL2023-156).

References

[1] M. Alles, E. Aljalbout, Learning to Centralize Dual-Arm Assembly, Frontiers in Robotics and AI 9(2022) 830007-830007.
[2] K. Nottensteiner, A. Sachtler, A. Albu-Schäffer, Towards Autonomous Robotic Assembly: Using Combined Visual and Tactile Sensing for Adaptive Task Execution, Journal of Intelligent & Robotic Systems 101(3)(2021) 49.
[3] K. Sharma, V. Shirwalkar, P.K. Pal, Peg-In-Hole search using convex optimization techniques, The Industrial Robot 44(5)(2017) 618-628.
[4] P. Liu, T. Qin, W.-W. Yu, B. Li, Task planning and experiment of robot auto-locking screw, Industrial Robot (9)(2022) 52-56.
[5] Z. Li, H.-S. Yu, H.-R. Wu, X.-X. Meng, Workpiece Grasping of Manipulator Based on Improved RRT Algorithm and Visual Positioning, Modular Machine Tool & Automatic Manufacturing Technique (12)(2022) 148-153.
[6] Y.-X. Tian, F.-F. Wu, Application of Convolutional Neural Network Algorithm in Artifact Grabbing, Machine Tool & Hydraulics 48(15)(2020) 76-80.
[7] L.-J. Li, Q.-Z. Li, T. Liu, Research on Digital Assembly Collision Detection for Insertingand Fitting Parts of Aircraft, Machinery Design & Manufacture (2)(2020) 145-148.
[8] H. Liu, Construction and Implementation of Hidden Markov Model, Journal of Shanghai University of Electric Power 37(5)(2021) 467-470.
[9] Z.-Y. Qin, P.-H. Chen, D.-Q. Jin, Existence of stationary solution of Amari dynamical neural field with ReLU function, Journal of Guangxi University (Natural Science Edition) 46(1)(2021) 231-235.
[10] Z.-Y. Huang, H.-L. Wu, Z. Wang, H. Li, DQN Algorithm Based on Averaged Neural Network Parameters, Computer Science 48(4)(2021) 223-228.
[11] J. Zhou, X.-L. Ding, Z. Lu, 3-D Dynamic Simulation and Experiment for Shaft and Hole Mating of Redundant Dual-arm Robot, Robot 28(4)(2006).